

Supporting information

Spin-coated fluorinated PbS QD superlattice thin film with high hole mobility

Pan Xia,¹ Daniel W. Davies,² Bijal B. Patel,² Maotong Qin,³ Zhiming Liang,⁴ Kenneth R. Graham,⁴ Ying Diao,² and Ming Lee Tang^{1,*}

¹ Department of Chemistry & Materials Science and Engineering Program, University of California, Riverside, 900 University Avenue, Riverside, California 92521, United States

² Department of Chemical and Biomolecular Engineering, University of Illinois at Urbana–Champaign, 600 South Mathews Avenue, Urbana, Illinois 61801, United States

³ Department of Materials Chemistry, School of Chemistry and Materials Science, University of Science and Technology of China, NO. 96 Jinzhai Road, Hefei, Anhui, 230026 P. R. China

⁴ Department of Chemistry, University of Kentucky, Lexington, Kentucky 40506, United States

1) Experimental Section

a) Chemicals

Lead (II) oxide (99.9995%) and silver nitrate (AgNO₃, 99.9995%) are from Alfa Aesar. dodecylamine (98%), 1,2-ethanedithiol (EDT) (>98%), ethanol (anhydrous, ≤0.005% water), 3-mercaptopropyl trimethoxysilane (3-MPTMS, 95%), 1H,1H,2H,2H-Perfluorodecyltriethoxysilane (PFDTEOS, 97%), phenyl isothiocyanate (98%), oleic acid (OA, 90%), 1-octadecene (ODE, 90%) and tetrabutylammonium hexafluorophosphate (TBA-PF₆, ≥99.0%), were purchased from Sigma-Aldrich and used as received. Hexanes was purchased from Fisher Scientific and dried with MgSO₄ before use. Toluene and acetonitrile were purified and dried with JC Meyer Solvent purification system. [NMe₄][SCF₃] is synthesized as our previous report.¹ Syntheses and cleaning of quantum dots (QDs) and fabrication and measurement of TFTs were carried out in nitrogen filled gloveboxes.

b) PbS QD synthesis

PbS QDs were synthesized and cleaned entirely in a glovebox, using a 1-dodecyl-3-phenylthiourea precursor in combination with lead oleate at 120°C, according to procedures first outlined by Hendricks and Owen². *N*-dodecyl-*N'*-phenylthiourea was prepared by adding *n*-dodecylamine (5.78 g, 31.2 mmol) in toluene (10 mL) and phenyl isothiocyanate (4.22 g, 31.2 mmol) in toluene (10 mL), producing a white powder. After vacuum filtration, the white solid is further dried under high vacuum for 4 hours. In a typical synthesis, lead oleate (1.41 g, 2.29 mmol) and ODE (14.75 ml) were mixed in 24 mL vials and heated to 120 °C in a nitrogen glovebox. 1-dodecyl-3-phenylthiourea (0.49 g, 1.53 mmol) and diglyme (0.5 ml) was mixed in 4 ml glass vials and is heated to 120 °C. Once the temperature is stable (15 minutes), the solution of thiourea was quickly added into the clear colorless solution. The reaction was quenched with a large amount of cold hexane after 10 minutes. The PbS QDs were thoroughly cleaned in glove box with three precipitation/redispersion steps using anhydrous ethanol as a bad solvent and anhydrous hexane as good solvent. Finally, QDs were dispersed in anhydrous toluene with a concentration of 72 μM, and optical absorption was performed to determine the QD size (5.1 nm according to the sizing curve of Moreels *et al.*³).

c) *Ligand Exchange*

OA and $\ominus\text{SCF}_3$ capped PbS QDs (molar ratio of OA: $\ominus\text{SCF}_3 = 2:1$) (PbS–OA+ SCF_3) are synthesized via partial ligand exchange with OA capped PbS QD with $[\text{NMe}_4][\text{SCF}_3]$.¹ Briefly, 0.68 ml PbS QDs in toluene ($[\text{PbS}] = 0.072 \text{ mM}$) is mixed with 52 μL $[\text{NMe}_4][\text{SCF}_3]$ acetonitrile solution (concentration of $[\text{NMe}_4][\text{SCF}_3] = 6.9 \text{ mg/ml}$). 0.65 ml toluene is added such that $[\text{PbS}] = 0.035 \text{ mM}$ in the mixture and molar ratio of $[\text{NMe}_4][\text{SCF}_3]$ to PbS QD = 40. This is stirred for 40 mins at room temperature. Under these conditions, one third of OA is replaced with $\ominus\text{SCF}_3$ (ligand replacement was measured by NMR in our previous work¹). The QDs were filtered with a Minisart SRP (Hydrophobic PTFE) syringe filter with 0.2 μm pore size. Then 1.5 ml acetone is added to precipitate the PbS QDs by centrifuging at 7830 rpm for 10 mins. The supernatant was removed, and 1.0 ml toluene used to redisperse the QDs such that $[\text{PbS}] = 0.050 \text{ mM}$.

d) *Fabrication of 3-MPTMS and perfluoro SAM*

Glass and silicon wafers were treated with 3-MPTMS or 1H,1H,2H,2H-Perfluorodecyltriethoxysilane as described previously.⁴ Glass and the silicon wafers were cleaned with fresh piranha solution (volume ratio of $\text{H}_2\text{SO}_4 : \text{H}_2\text{O}_2 = 3:1$) for 20 minutes. 3mM 3-MPTMS in trichloroethylene was dropcast on the clean and dry surface. After 10 seconds, the substrate was spin coated at 3000 rpm for 30s, then placed in a saturated ammonia environment under static vacuum overnight. After 8 hours, the thin films were sonicated in toluene to remove any physically adsorbed 3-MPTMS.

e) *Spin-coating PbS–SCF₃ thin film*

These partially ligand-exchanged colloidal PbS QD were drop-cast in a nitrogen glovebox on substrates (like silicon wafers with either thermal or native oxides, glass and silicon dioxide TEM grids) coated with self-assembled monolayers (SAMs), e.g. 3-MPTMS. 3-MPTMS serves to promote the adhesion of the PbS QDs to silicon dioxide. The 3-MPTMS treatment or PFDTEOS treatment (denoted as perfluoro treatment) of substrate is described before. Two consecutive ligand exchanges were performed on this thin film, where 2 mg/ml of $[\text{NMe}_4][\text{SCF}_3]$ in acetonitrile was allowed to equilibrate for 5 minutes on the QD thin film. Excess ligand was removed by spin-coating, followed by three washing steps: twice with ethanol and finally with tetrahydrofuran. ATR-IR measurements of PbS– SCF_3 verify the complete removal of OA after two cycles of ligand exchange in thin film.

f) *Dip-coating PbS–SCF₃ thin film*

The PbS–OA QDs were dropcast on glass (with 3-MPTMS treatment) for optical samples to get a thicker thin film spincoated on silicon wafer to fabricate a homogenous thin film for transistor. The film is soaked in 2 mg/ml $[\text{NMe}_4][\text{SCF}_3]$ acetonitrile solution for 15 mins to completely remove OA, then rinsed with acetonitrile twice. Acetonitrile is removed by spinning the substrate at 1500 rpm and cleaned twice with ethanol and once with tetrahydrofuran (removed by spinning wafer on the spin coater chuck).

Table S0. Fabrication methods of PbS–ligand thin film

Method	0	1	2	3	4	5
Abbreviation	PbS-OA dipcoat	PbS-SCF ₃ dipcoat	PbS-SCF ₃ dipcoat	PbS-SCF ₃ superlattice		
Solution LX ^[1]	NO	NO	NO	YES		
NC before film deposition	PbS-OA	PbS-OA	PbS-OA	PbS-SCF ₃ +OA		
Substrate pretreatment	3-MPTMS				Perfluoro SAM	
Measurement	Optical	Optical, TFT, AFM, GISAXS		Optical, TFT, AFM, TEM, GISAXS	TFT, TEM, GISAXS	TFT
Thin film NC deposition	dropcast	dropcast	spincoat	spincoat		
Solid LX	NO	dip		spin		
Repeat solid LX	NO	NO	NO	YES	YES	YES
Annealing ^[2]	NO	NO	NO	NO	YES	NO

Note:

[1] LX is the abbreviation of ligand exchange.

[2] Annealing temperature is at 60 °C. The annealing temperature could be further optimized to get higher carrier mobility. However, in-situ TEM experiments of Baik et al's work⁵ indicate that PbS QDs don't merge when annealing PbS QD thin film less than 70 °C for 30 minutes. Thus, to be safe, we annealed at 60°C. We wanted to anneal for longer time to remove remaining solvents slowly but completely. Thus, we lowered the annealing temperature to remove extra solvents but also decrease the possibility of nanoparticles fusing.

g) *Optical Characterization*

The absorption spectra of solution were obtained with a Jasco/V670 UV/Vis absorption spectrophotometer. The absorption spectra of thin films were obtained with a Varian Cary 500 UV/Vis/NIR spectrophotometer. Photoluminescence of the QDs both in solution and thin film are obtained with a Bayspac SuperGamutTM NIR Spectrometer using 488 nm laser (OBIS LS, Coherent) excitation. Thin film samples for absorption and emission are fabricated by spincoating the PbS QD solution on glass after 3-MPTMS treatment and sealed with epoxy to keep the sample air-free. The AFM images were obtained by a Dimension Icon XR (Bruker) in tapping mode. IR spectra were obtained on a Nicolet iS10 IR Spectrometer (Thermo Fisher Scientific) in transmission mode.

h) *Grazing incidence small angle x-ray scattering (GISAXS)*

GISAXS experiments were performed at beamline 12-ID-B of the Advanced Photon Source at Argonne National Laboratory. The PbS QD solution was spincoated onto an atomically smooth silicon wafer with a native oxide treated with 3-MPTMS. Samples were sealed under an inert atmosphere during transit to the beamline and exposed to ambient air for several minutes prior to and during scanning. Spectra were collected on a Pilatus 2M, two-dimensional detector using an incident X-ray beam energy of 13.3 keV and a sample to detector distance of 3.6m, calibrated against a silver behenate standard. Spectra collected at incident angles ranging from 0.04° to 0.2°

show qualitatively similar features. Quantitative peak fitting was performed on spectra obtained using an incident angle of 0.12° , below the estimated critical angle of PbS (0.24° at 13.3 keV). Analysis was done by simulating the diffraction pattern using the GIXSGUI package⁶ for MATLAB by specifying the lattice parameters and orientation and performing iterative fitting to match the experimentally obtained scattering pattern.

i) *Transmission electron microscopy (TEM)*

40 nm thick SiO₂ films on silicon nitride TEM grids with 50 x 50 μm/24 apertures are from Ted pella, Inc. (part no. 21530-10). The PbS QD solution prepared as above was spincoated on these TEM grids after 3-MPTMS treatment. TEM images were recorded on a FEI Titan Themis 300 with an X-FEG electron gun. The superlattice spacing were determined from multiple regions by analyzing the scattering peak positions extracted from the Fourier-transformed images.

j) *Cyclic Voltammetry*

Cyclic voltammetry (CV) electrochemical measurements were conducted on a WaveDriver 10 Potentiostat (WD10/BASIC, Pine Research Instrument). Measurements were performed under nitrogen in anhydrous acetonitrile with 0.1 M TBA-PF₆ as the supporting electrolyte. A 0.5 mm platinum electrode (part no. RRP257PT, Pine Research Instrument) served as the working electrode and counter electrode. An encased Silver (Ag) pseudo-reference electrode with ceramic frit on bottom filled with a 10 mM AgNO₃, 0.1 M TBA-PF₆, acetonitrile solution served as the reference electrode (part no. RREF0153, Pine Research Instrument). The concentration of [NMe₄][SCF₃] in solution was approximately 3 mM. CV scans were performed at 100 mV/s, and half-peak potentials ($E_{p/2}$) were used to estimate the oxidation potential, $E^{o}_{1/2}$, as the CV of [NMe₄][SCF₃] is irreversible due to dimerization of the thiolate groups.⁷ An internal standard, ferrocene is added to the electrochemical cell after CV was performed on [NMe₄][SCF₃]. The ferrocene/ferrocenium (Fc/Fc⁺) redox couple with a value of 4.8 eV with respect to vacuum. The HOMO of [NMe₄][SCF₃] is measured as $-(E_{1/2, [NMe_4][SCF_3]} - E_{1/2, ferrocene}) + 4.8$ eV.⁸ The potential of this Ag/AgNO₃ standard electrode in 0.01 M acetonitrile vs. saturated calomel electrode (SCE) is +0.3 V.⁹ Therefore the $E_{p/2}$ of [NMe₄][SCF₃] is +0.69 V vs. SCE, which is lower than thiophenols and aryl disulfides reported by Nicewicz et al.⁷

k) *Ultraviolet Photoelectron Spectroscopy (UPS)*

The substrates for the UPS measurement are on 1.5 cm × 1.5 cm native silicon wafer coated with a 60 nm Au layer formed by thermal evaporation. The PbS–SCF₃ QD thin film was fabricated as described above, resulting in a QD film thickness of ~40–50 nm. The films were fabricated in a glovebox at UC Riverside, shipped in nitrogen filled sealed packages to the University of Kentucky, unpacked in a nitrogen-filled glovebox and inserted into the ultra-high vacuum system directly through the glovebox without ever being exposed to the atmosphere. An Excitech H Lyman-α photon source (E-LUX™121) coupled with a 90° ellipsoidal mirror (E-LUX™ EEM Optical Module) was used as the excitation source for UPS with an 8 Torr nitrogen purge of the beam path. The photoelectrons were detected with an 11-inch diameter hemispherical electron energy analyzer coupled with a multichannel plate detector using a 5 eV pass energy. A negative 5 V bias was applied to the samples during measurements. The SECO (ionization energy) of the samples was determined by the intersection of the background and a linear fit to the lower 50% of the SECO as we described in our previous publication.¹⁰

1) TFT Fabrication and Characterization

Current-voltage transistor measurements were performed in air-free conditions in bottom contact geometry with a common gate separated by a 200 nm dry thermal oxide patterned with 35 nm Au electrodes on a 5 nm Ti adhesion layer. The Keithley 2636B semiconductor parameter analyzer was used for all measurements with a Signatone probe station. The channel lengths, L are 10, 20, 30 and 100 μm . The ratio of channel width, W , to L , or $W/L = 20$ in all cases. The scan rate is 0.09-0.10 V/ms to minimize the influence of trap induced transient decays of the measured current. The annealed sample was heated on a KW-4A hotplate at 60°C for 3 hours in a nitrogen glovebox.

2) Supporting Data

a) Electronic absorption and photoluminescence of partially PbS/(OA+SCF₃) QDs
OA capped PbS QDs were ligand exchanged in a mixture of toluene and acetonitrile with [NMe₄][SCF₃] to replace one third of OA with $\ominus\text{SCF}_3$ ligands. Optical characterization of this partial-ligand-exchanged PbS QD, PbS-OA+SCF₃ is shown in Figure S4.

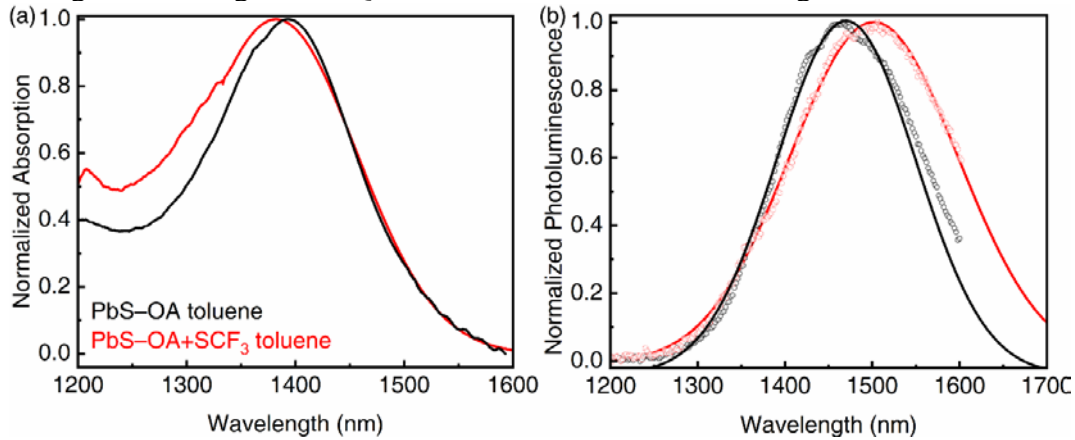


Figure S1. (a) Optical absorption and (b) photoluminescence (PL) of PbS QDs capped with OA, PbS-OA (black) and PbS-SCF₃+OA (red, OA: SCF₃ = 2:1) in toluene with 488 nm excitation. The blue shift of the 1st exciton peak and red shift of the PL are in agreement with our previous work on PbS QDs with diameter=3.8nm.¹

b) Simulated GISAXS diffraction peaks by using GIXSGUI

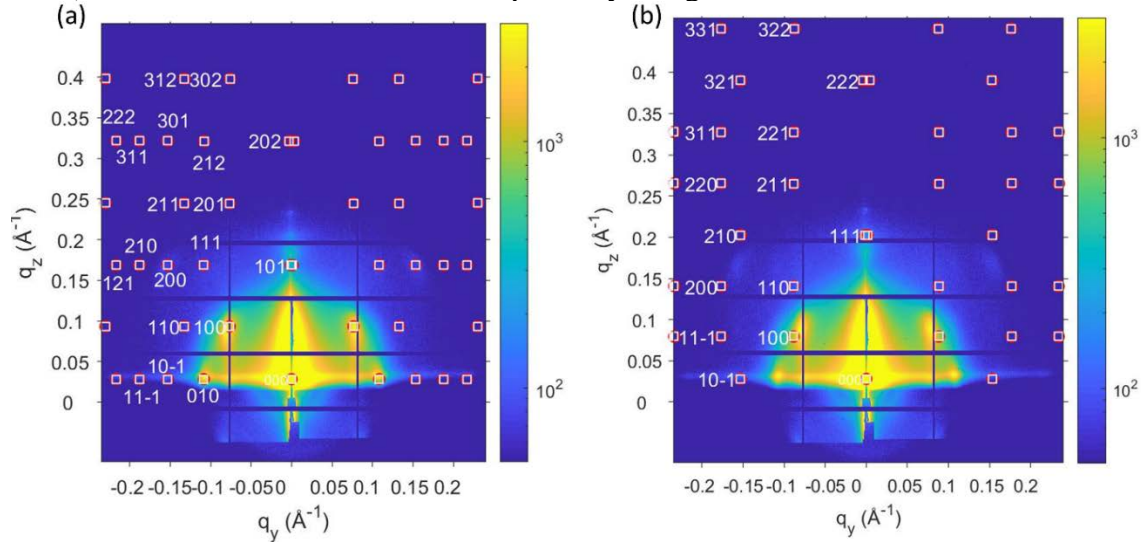


Figure S2. Simulated diffraction peaks overlaid on the experimental diffraction pattern for spin-coated films without annealing. The diffraction pattern was simulated as a cubic unit cell with the (a) (101) or the (b) (111) plane parallel to the substrate. A symmetry of P_1 was used to calculate all possible peak positions without considering the specific symmetry of the lattice. Due to limited number of peaks, space group and symmetry could not be determined.

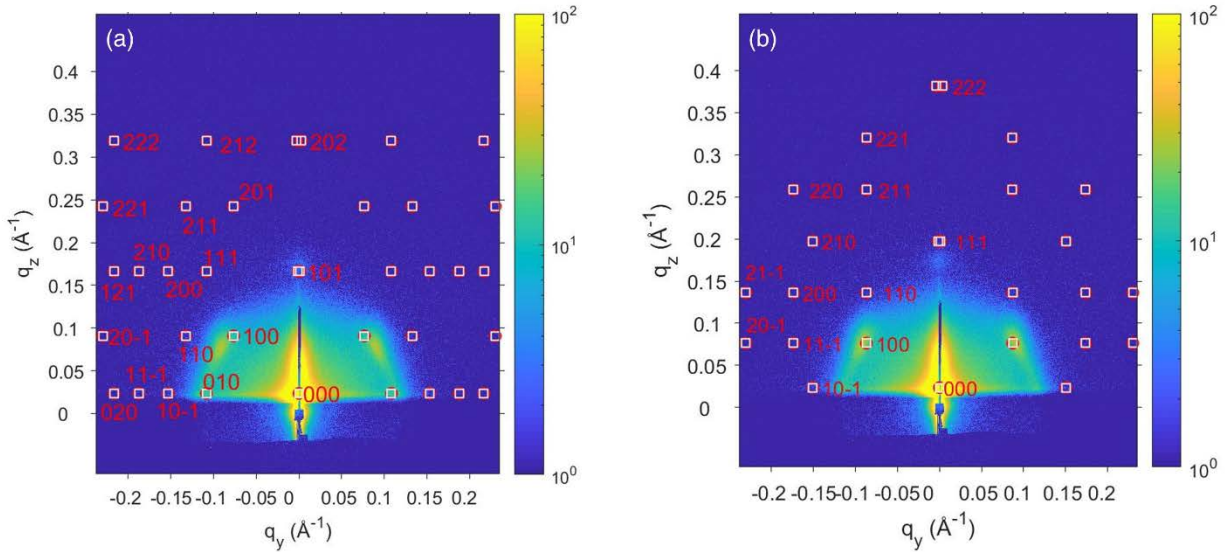


Figure S3. Simulated diffraction peaks overlaid on the experimental diffraction pattern for dipcoated films without annealing. The diffraction pattern was simulated as a cubic unit cell with the (a) (101) or the (b) (111) plane parallel to the substrate. A symmetry of P_1 was used to calculate all possible peak positions without considering the specific symmetry of the lattice.

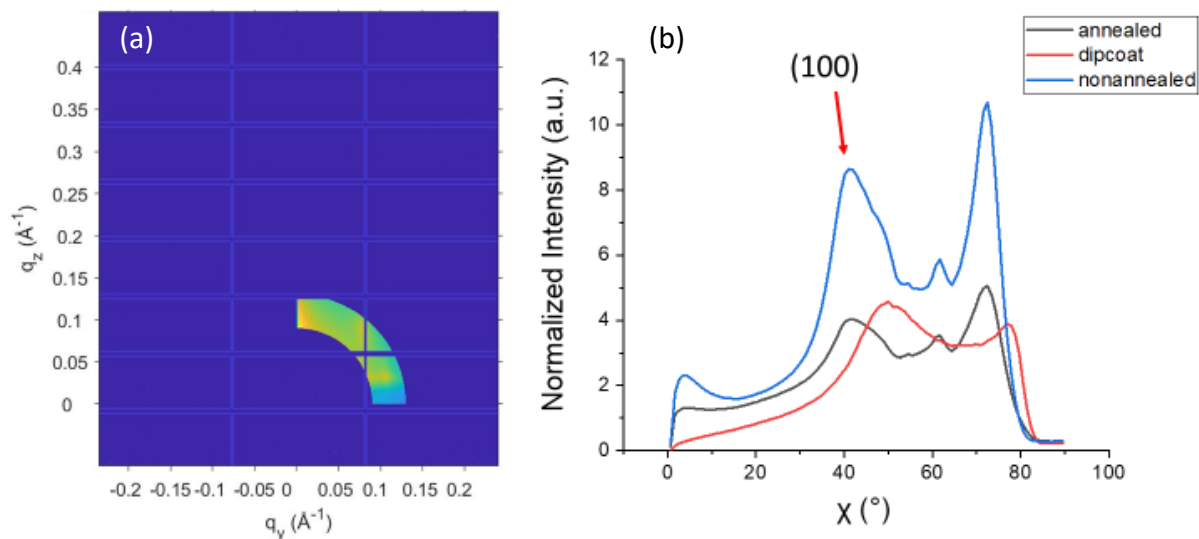


Figure S4. (a) Plotted region mask and (b) reshaped χ -Q plot comparing the normalized intensity among the annealed and nonannealed spincoated thin film, and the dipcoated PbS@SCF₃ thin film. The intensities were normalized with respect to the exposure time and sample thickness. We also made a geometric correction to the intensity through multiplying by a factor of $\sin(\chi)$.

c) Transmission electron microscopy characterization of PbS–SCF₃ superlattice film

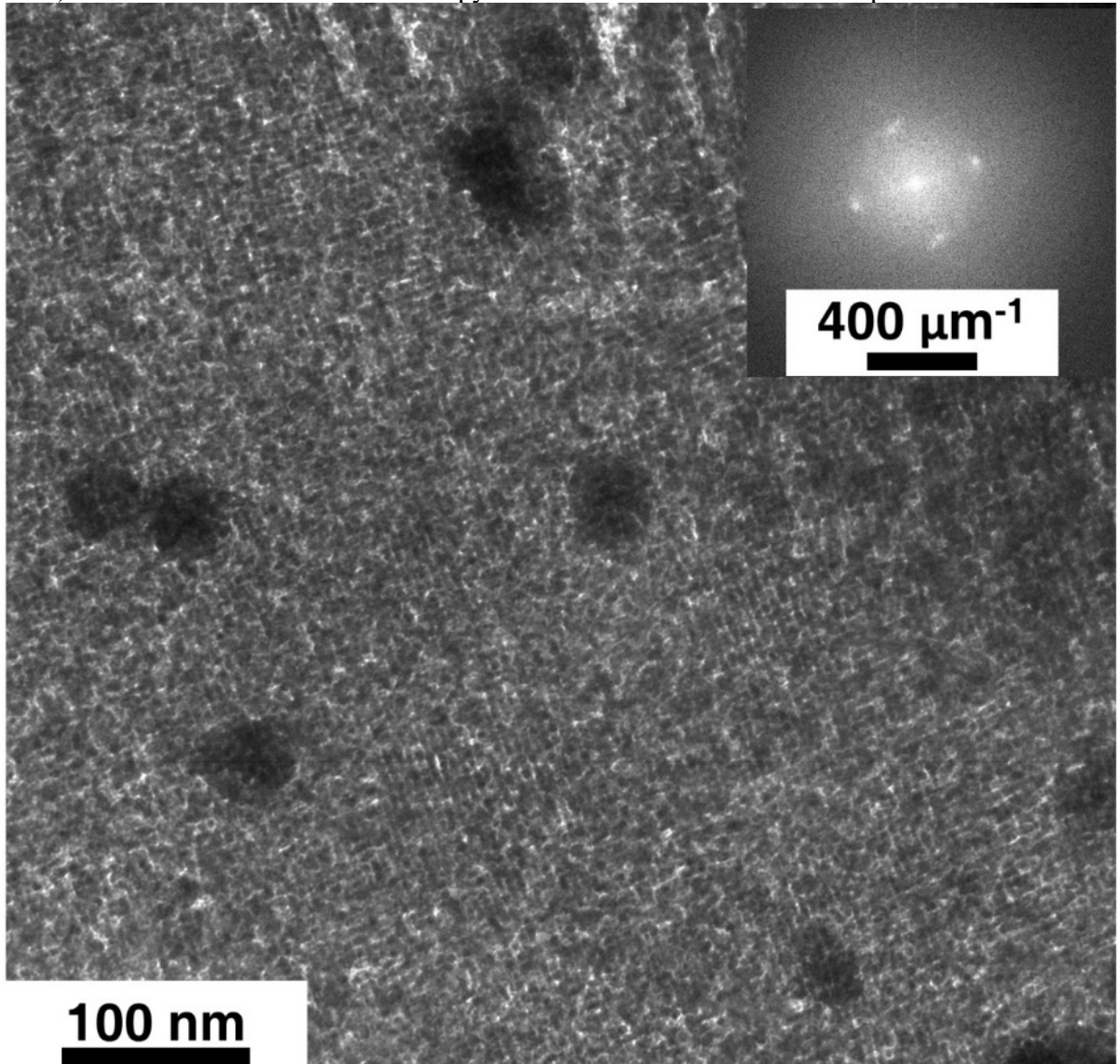


Figure S5. TEM image of PbS–SCF₃ QD superlattice (Method 3 Table S0) with local area 650 nm x 650 nm. The insert is the corresponding FFT image with two pairs of scattering spots stemming from long range order of the QDs. There are some polymeric impurities visible.

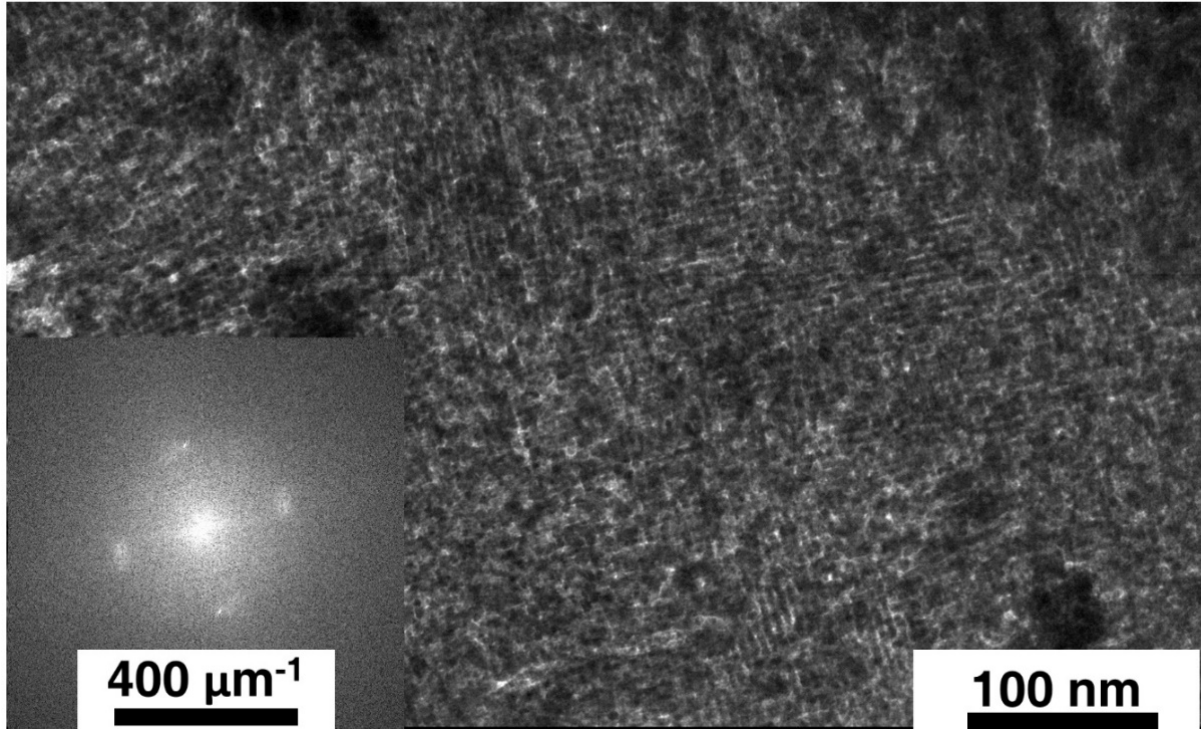
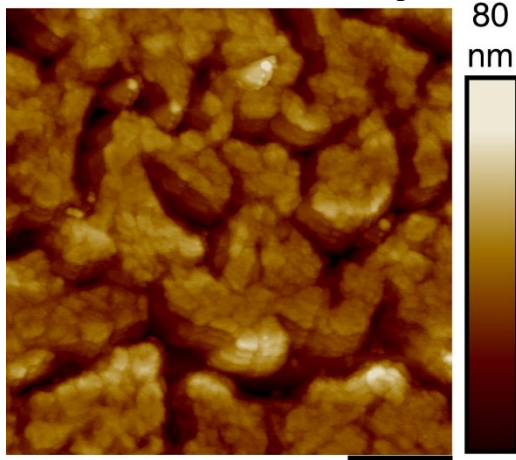


Figure S6. Additional TEM images of the PbS QD superlattice (method 3 Table S0) with local area 760 nm x 300 nm. The insert is the corresponding FFT image with two pairs of scattering spots.

d) Atomic force microscope (AFM) images



RMS= 12.1 nm

1.0 μm

Figure S7. AFM images of unannealed dipcoated PbS-SCF₃ QD thin films (Method 2 Table S0).

e) Thin film field-effect transistor measurements

PbS-EDT thin film transfer and output curves

PbS QDs is spincoated on 3- MPTMS treated silicon wafer with a thermal oxide. As described Section 1e), an EDT solution is pipetted on the PbS QD film to replace OA ligands. Extra EDT is spun away after waiting for 5 minutes to complete the ligand exchange. Dimethyl sulfoxide (DMSO) is added to remove remaining EDT and then THF is added to the thin film to remove OA. We found that PbS-EDT films being fabricated via solid ligand exchange have no significant difference in carrier mobility and on off ratio whether this exchange is performed once or twice.

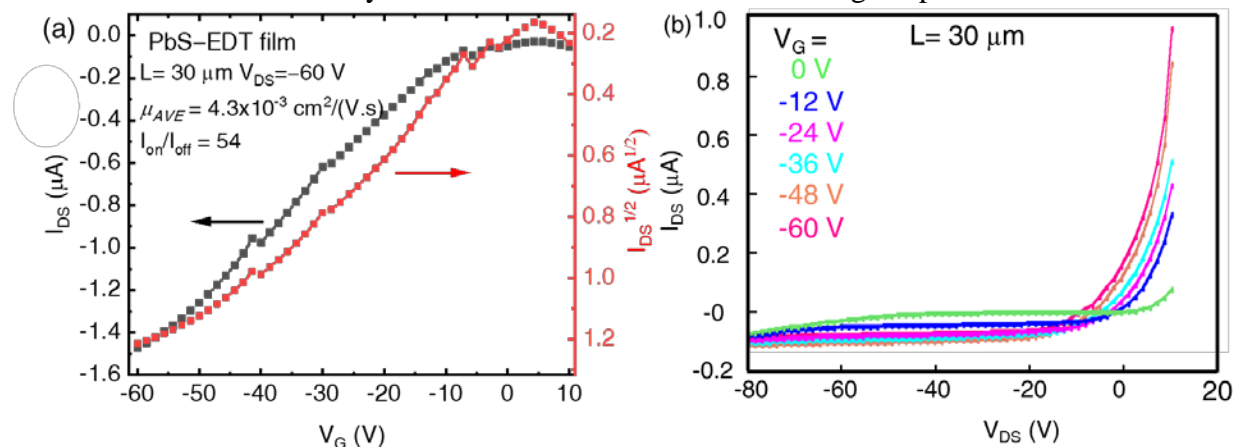


Figure S8. PbS-EDT TFTs only show hole transport in the a) transfer and b) output curves via a one-time solid ligand exchange.

Average hole mobilities μ_{AVE} were calculated from transfer curves acquired at source drain voltage, $V_{DS} = -70/ -80$ V, in the saturation regime with equation:

$$\mu = \left(\frac{\partial \sqrt{|I_{DS}|}}{\partial V_G} \right)^2 \frac{2L}{WC_i} \quad \text{Equation S2}$$

Where W is the channel width, L is the channel length, and C_i is the capacitance per unit area of the gate oxide. The carrier mobilities reported here are averages of 3–5 devices.

The I-V curves are non-ideal with two slopes. Here, two slopes are used to calculate the carrier mobility as described by Phan *et al* and Choi *et al*.^{11, 12} Since the gate voltages, V_G , can be scanned from positive to negative, or vice-versa, we plot four mobility values. Considering the crystalline domains of the PbS QD superlattice are on the order of the channel lengths, it is not surprising that there is some deviation between devices. However, annealed PbS QD thin films fabricated on 3-MPTMS thiol SAMs only show one slope, unlike the TFTs presented in Fig. S12 below.

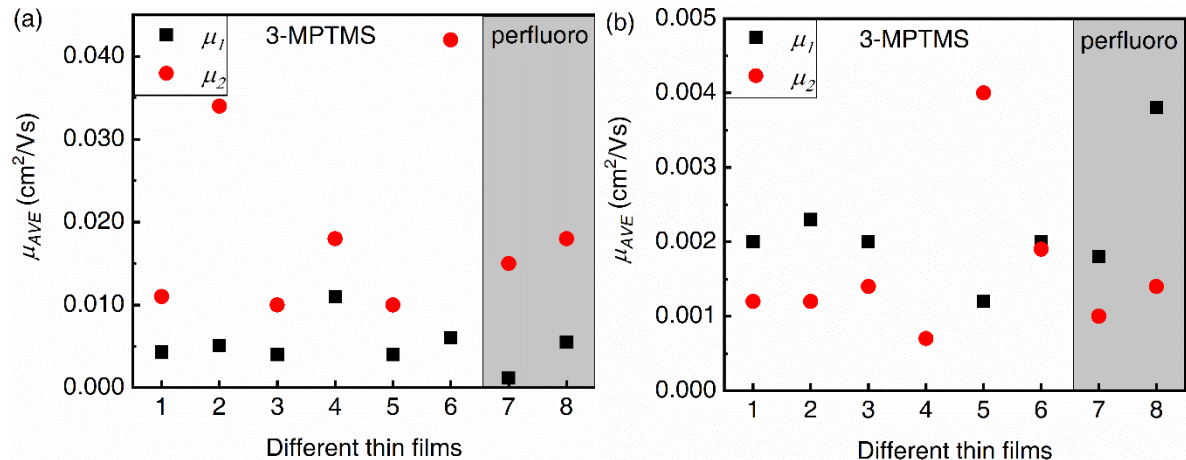


Figure S9. Hole mobilities of TFTs with different SAMs on the dielectric (3-MPTMS and perfluoro), sweeping V_G from negative to (a) positive and (b) vice-versa.

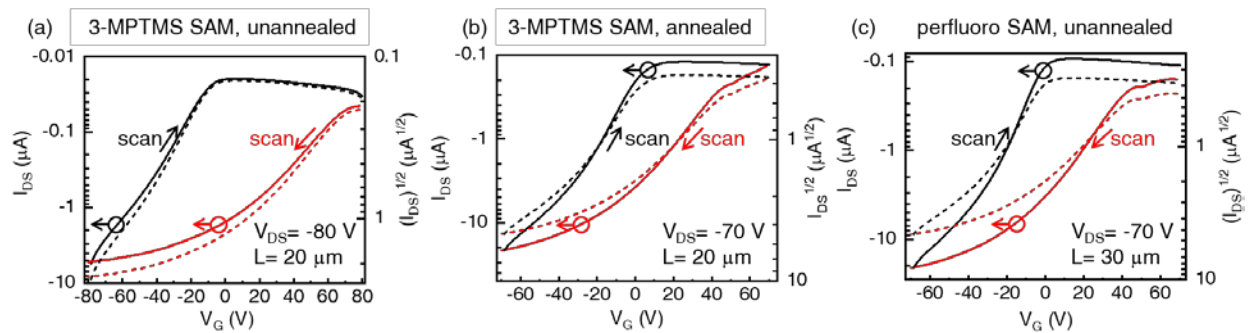


Figure S10. Representative transfer curves from PbS-SCF₃ QD superlattice thin films. The red and black traces represent scanning towards negative and positive gate voltages (V_G) respectively. (a) and (b) represent TFTs with dielectric modified with 3-MPTMS, while (c) has the dielectric modified with a perfluoro SAM. Sample (b) has been annealed at 60°C. The same data is presented with linear I_{DS} in Fig. 5.

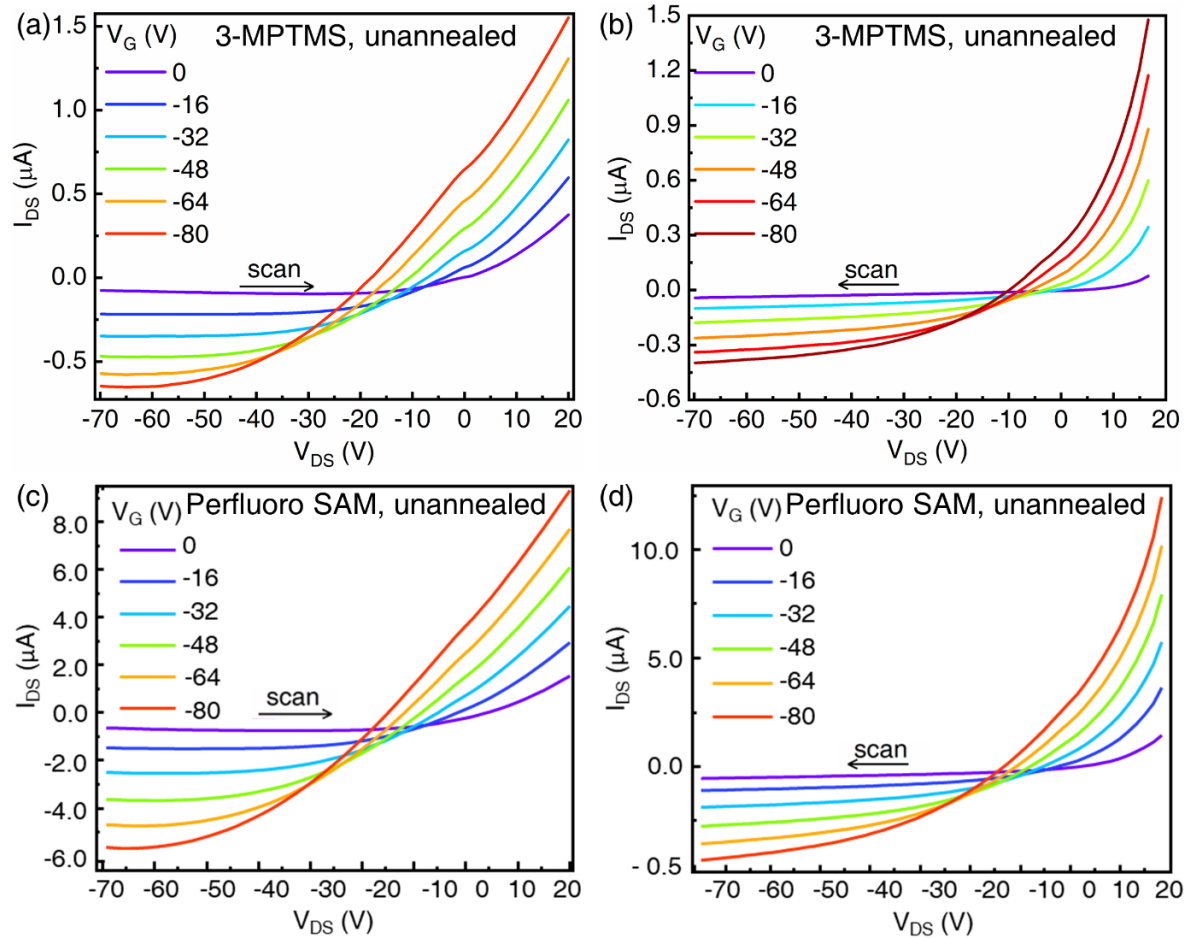


Figure S11. Typical output curves of spincoated unannealed PbS-SCF₃ QD thin film transistors (TFTs) with (a, b) 3-MPTMS self-assembled monolayer (SAM) and (c, d) perfluoro SAM treatment on the dielectric. Arrows indicate the direction V_{DS} is swept.

PbS–SCF₃ film fabricated via dipcoating (Method 2 Table S0)

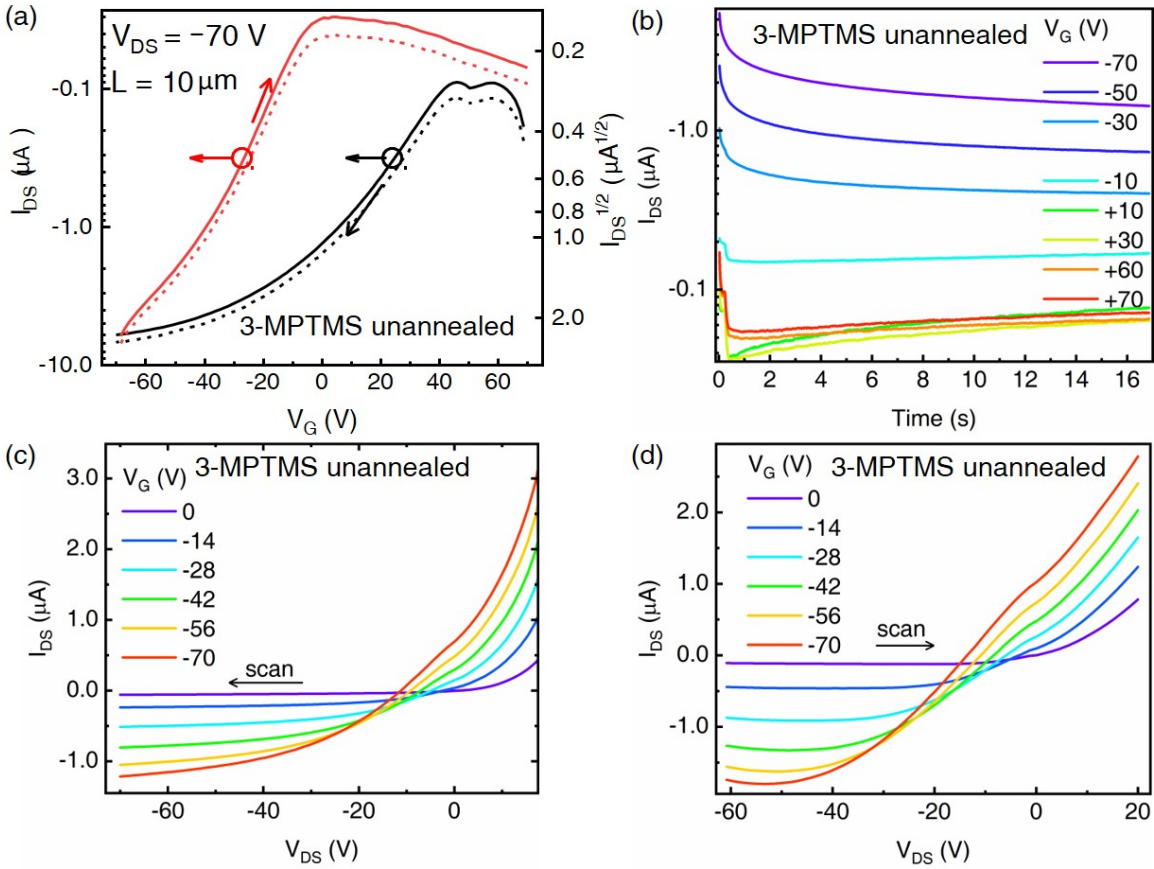


Figure S12. Representative transfer and output curves of dipcoated PbS–SCF₃ QD FETs with 3-MPTMS SAM on dielectric. Channel length is 10 μm. (a) Transfer curves (solid line) with source drain voltage, V_{DS} , is kept at -70 V. The dash line is the square root of the source drain current, I_{DS} . (b) Bias stress curves of the dipcoated PbS–SCF₃ QD thin films where $V_{DS} = -70$ V and the gate voltage, V_G is varied. Output curves sweeping from (c) negative to positive V_{DS} and (d) positive to negative V_{DS} .

Table S1. Summary of transistor performance, including the maximum and average mobilities, μ_{MAX} and μ_{AVE} , the threshold voltage, V_T , and the on/ off ratios, I_{ON} / I_{OFF} corresponding to dipcoated PbS–SCF₃ film transistor in Figure S12.

Channel length (μm)	30		20		20	
	+ V_G	- V_G	+ V_G	- V_G	+ V_G	- V_G
Scan towards	+ V_G	- V_G	+ V_G	- V_G	+ V_G	- V_G
μ_{AVE} [cm ² /Vs]	0.006	0.003	0.007	0.003	0.006	0.002
μ_{MAX} [cm ² /Vs]	0.020	0.005	0.023	0.005	0.019	0.004
I_{ON} / I_{OFF}	200	100	200	100	200	100
V_T [V]	-10	+30	-10	+40	-15	+50

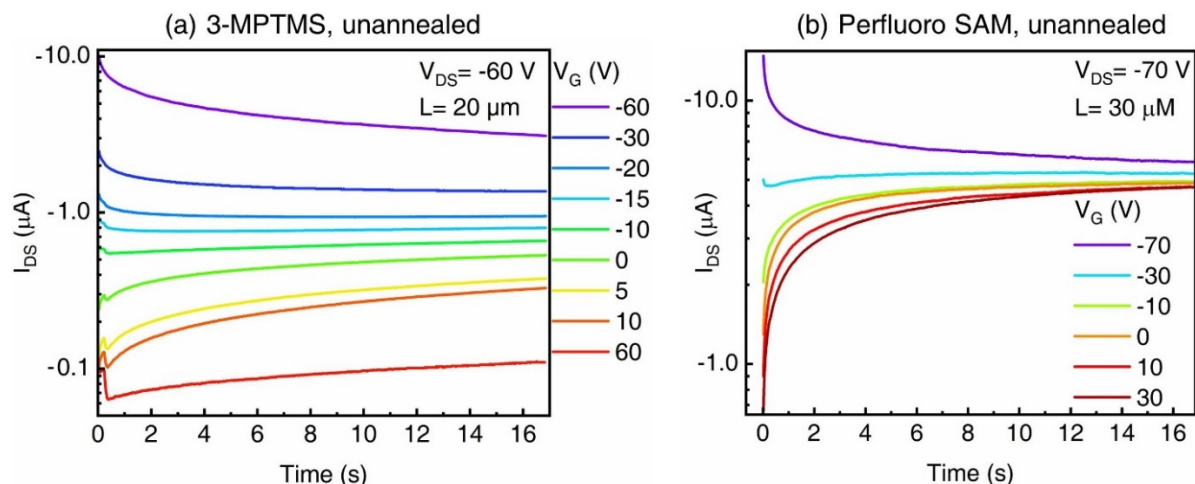


Figure S13. Bias stress curves for unannealed PbS-SCF₃ QD thin films spin-coated on (a) 3-MPTMS treated or (b) perfluoro treated dielectric (b) where $V_{DS} = -60$ and -70 V respectively as the gate voltage, V_G is varied. In both 3-MPTMS treated or perfluoro treated substrate, the source drain current, I_{DS} , decreases in magnitude over time, indicating that the hole current is trapped and not related to the dielectric treatment.

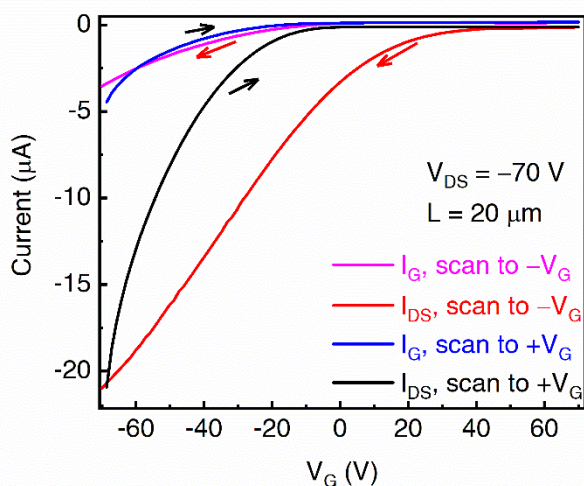


Figure S14. Representative transfer curves (red and black) of PbS-SCF₃ QD thin films annealed at 60°C with 3-MPTMS SAM on dielectric with the gate leakage current, I_G included (blue and magenta).

f) Ultraviolet photoelectron spectroscopy (UPS)

The conduction band (CB) minimum, E_C , is estimated by adding the energy of the valence band (VB) maximum, optical band gap, E_g^{opt} and the Coulombic stabilization energy of the confined electron and hole as described previously.¹³

$$E_C = E_V + E_G^{opt} + 1.786 \frac{e^2}{4\pi\epsilon_0\epsilon_{QD}R} \quad \text{Equation S1}$$

where e is the charge of the electron, ϵ_0 is the permittivity of free space, ϵ_{QD} is the optical dielectric constant of the QD core material, and R is the quantum dot radius (determined by matching the first absorption peak in solution to a published sizing curve³).

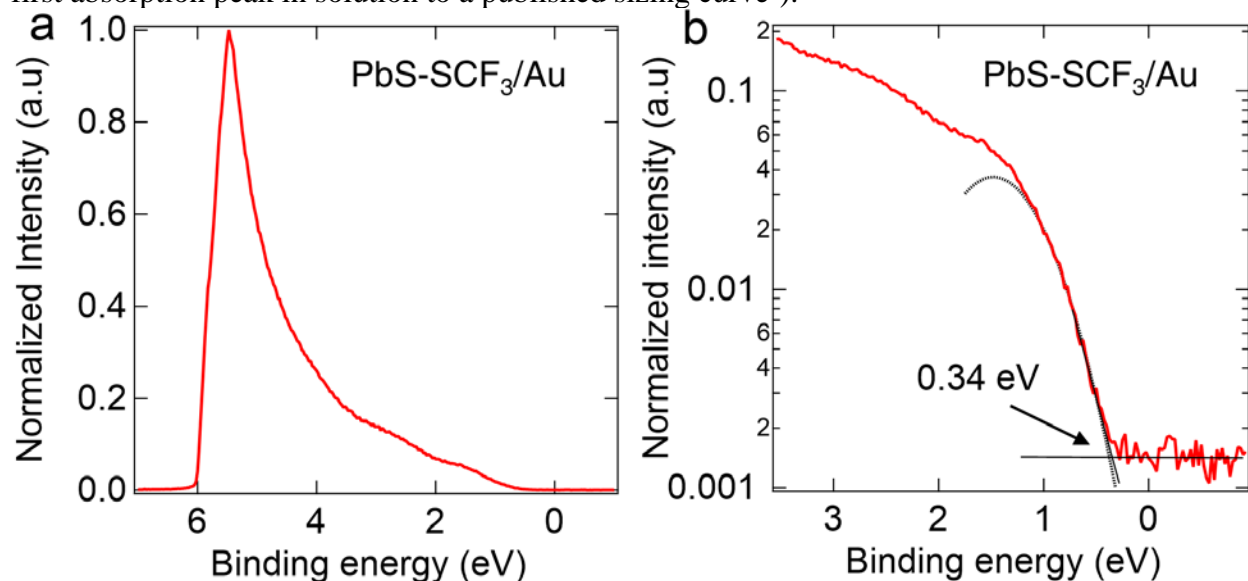


Figure S15. UPS spectra measured with a 10.2 eV H Lyman- α lamp of PbS-SCF₃ QD thin films on gold coated silicon wafer. (a) Complete spectra on a linear scale, which clearly shows the secondary electron cut-off region, and (b) the valence band onset region on a semi-log plot.

Table S2. Parameters of UPS samples of PbS-SCF₃ thin film on gold coated substrate. The lack of a well-defined valence band (VB) onset in the UPS measurements and the use of a logarithmic plot to extract the VB onset introduces some uncertainty (*ca.* ± 0.1 eV) due to the assignment of the background level. For example, different UPS systems will have different signal to noise ratios that will likely influence where the background intersects the parabolic fit. The work function (Φ), VB maximum (E_V), and VB onset relative to the Fermi energy are obtained from Figure S8. E_g^{opt} is the optical bandgap from optical absorption spectra. Coulombic stabilization energy (eV) of the confined electron and hole and energy of conduction band (CB) minimum (E_C) are calculated with Equation S1.

Sample	Substrate	Φ (eV)	VB onset (eV)	E_V (eV)	$\lambda_{max}^{[1]}$ (nm)	E_g^{opt} (eV)	Coulombic stabilization energy (eV)	E_C (eV)
PbS-SCF ₃ /Au	Au	4.20	0.34	-4.54	1420	0.87	0.085	-3.58

[1] λ_{max} is the first exciton absorption maximum of dipcoating PbS-SCF₃ film.

g) Cyclic voltammetry (CV) measurements

The CV of $[\text{NMe}_4][\text{SCF}_3]$ in acetonitrile is irreversible due to dimerization of the thiolate groups.⁷ Half-peak potentials ($E_{p/2}$) were used to estimate the oxidation potential, $E^{\circ}_{1/2}$. The $E_{p/2}$ of $[\text{NMe}_4][\text{SCF}_3]$ is +0.99 V vs. Ag/AgNO_3 nonaqueous reference electrode (Ag wire in 0.01 M AgNO_3 acetonitrile solution).

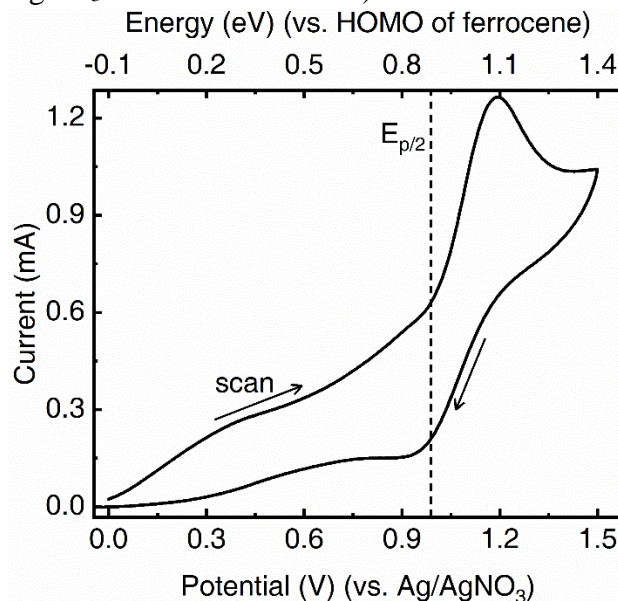


Figure S16. Cyclic voltammetry of $[\text{NMe}_4][\text{SCF}_3]$ in acetonitrile at room temperature (measurement details described in the experimental section). The highest occupied molecular orbitals (HOMO) of ferrocene with respect to vacuum is -4.8 eV. The dashed line shows the half peak potential ($E_{p/2}$) position of $[\text{NMe}_4][\text{SCF}_3]$.

References

1. P. Xia, Z. Liang, M. Mahboub, J. van Baren, C. H. Lui, J. Jiao, K. R. Graham and M. L. Tang, *Chem. Mater.*, 2018, **30**, 4943-4948.
2. M. P. Hendricks, M. P. Campos, G. T. Cleveland, I. Jen-La Plante and J. S. Owen, *Science*, 2015, **348**, 1226-1230.
3. I. Moreels, K. Lambert, D. Smeets, D. De Muynck, T. Nollet, J. C. Martins, F. Vanhaecke, A. Vantomme, C. Delerue, G. Allan and Z. Hens, *ACS Nano*, 2009, **3**, 3023-3030.
4. M. L. Tang, A. D. Reichardt, N. Miyaki, R. M. Stoltenberg and Z. Bao, *J. Am. Chem. Soc.*, 2008, **130**, 6064-6065.
5. S. J. Baik, K. Kim, K. S. Lim, S. Jung, Y.-C. Park, D. G. Han, S. Lim, S. Yoo and S. Jeong, *The Journal of Physical Chemistry C*, 2011, **115**, 607-612.
6. Z. Jiang, *J. Appl. Crystallogr.*, 2015, **48**, 917-926.
7. H. G. Roth, N. A. Romero and D. A. Nicewicz, *Synlett*, 2016, **27**, 714-723.
8. K. E. Knowles, M. Malicki and E. A. Weiss, *J. Am. Chem. Soc.*, 2012, **134**, 12470-12473.
9. L. Meites, *Handbook of analytical chemistry*, McGraw-Hill, New York, 1963.
10. Z. Liang, Y. Zhang, M. Sourji, X. Luo, Alex M. Boehm, R. Li, Y. Zhang, T. Wang, D.-Y. Kim, J. Mei, S. R. Marder and K. R. Graham, *J. Mater. Chem. A*, 2018, **6**, 16495-16505.
11. H. Phan, M. J. Ford, A. T. Lill, M. Wang, G. C. Bazan and T.-Q. Nguyen, *Adv. Funct. Mater.*, 2018, **28**, 1707221.

12. H. H. Choi, K. Cho, C. D. Frisbie, H. Siringhaus and V. Podzorov, *Nat Mater*, 2017, **17**, 2-7.
13. P. R. Brown, D. Kim, R. R. Lunt, N. Zhao, M. G. Bawendi, J. C. Grossman and V. Bulović, *ACS Nano*, 2014, **8**, 5863-5872.